molecules

MDPI

*Communication*

# Rigid Nanoporous Urea-Based Covalent Triazine Frameworks for C2/C1 and $CO_2/CH_4$ Gas Separation

**Chidharth Krishnaraj †, Himanshu Sekhar Jena *,†, Florence Lecoeuvre, Karen Leus and Pascal Van Der Voort ***

COMOC, Center for Ordered Materials, Organometallics and Catalysis, Department of Chemistry, Ghent University, 9000 Gent, Belgium; chidharth.krishnaraj@ugent.be (C.K.); florencelecoeuvre@gmail.com (F.L.); Karen.Leus@ugent.be (K.L.)

* Correspondence: himanshu.jena@ugent.be (H.S.J.); pascal.vandervoort@ugent.be (P.V.D.V.)

† These authors contributed equally to this work.

**Abstract:** C2/C1 hydrocarbon separation is an important industrial process that relies on energy-intensive cryogenic distillation methods. The use of porous adsorbents to selectively separate these gases is a viable alternative. Highly stable covalent triazine frameworks (urea-CTFs) have been synthesized using 1,3-bis(4-cyanophenyl)urea. Urea-CTFs exhibited gas uptakes of $C_2H_2$ (3.86 mmol/g) and $C_2H_4$ (2.92 mmol/g) at 273 K and 1 bar and is selective over $CH_4$. Breakthrough simulations show the potential of urea-CTFs for C2/C1 separation.

**Keywords:** covalent triazine frameworks; covalent organic frameworks; gas separation; C2/C1 hydrocarbon separation; $C_2H_2/CH_4$; $CO_2/CH_4$



**Citation:** Krishnaraj, C.; Jena, H.S.; Lecoeuvre, F.; Leus, K.; Van Der Voort, P. Rigid Nanoporous Urea-Based Covalent Triazine Frameworks for C2/C1 and $CO_2/CH_4$ Gas Separation. *Molecules* **2021**, *26*, 3670. https://doi.org/10.3390/molecules26123670

Academic Editor: Dongmei Cui

Received: 20 May 2021
Accepted: 15 June 2021
Published: 16 June 2021



## 1. Introduction

The separation of C1 and C2 gases is a critical process in many industrial activities. For example, acetylene is an important industrial byproduct of petroleum and natural gas processing, which needs to be separated. In addition, there are other industrial processes wherein ethylene and acetylene are produced by the oxidative and non-oxidative coupling of methane [1]. However, quite often the methane conversion remains incomplete and recovering the unreacted methane is essential [2]. As another example, in the process of extracting natural gas, methane needs to be separated from carbon dioxide [3]. Natural gas consists of high amounts of carbon dioxide that must be removed to obtain pure methane, which can be used as an energy source for fuels and chemicals. As a final example, the separation of $CO_2$ in flue gases (typically containing about 75% nitrogen and traces of water (vapor)) is becoming an important process in carbon capture and utilization CCU strategies.

Metal organic frameworks (MOFs) have been studied for this purpose [4–6]. Although some show very high adsorption capacities and selectivities, they often lack long-term stability, an important factor for a potential adsorbent [7]. Hence, other types of porous adsorbents, such as porous organic polymers are also considered for such gas separation processes.

Covalent triazine frameworks (CTFs) are a class of organic porous materials that can be used for gas separation [8–10]. Research on CTFs has boomed due to their ease of synthesis, tunable porosities, desirable functionalization, and ultra-high stability [11–14]. They are primarily made through an ionothermal synthesis, where $ZnCl_2$ is used as an ionic liquid solvent and catalyst for the trimerization of dinitrile linkers. The ionothermal synthesis method has so far been used to design several inherent functionalities in CTFs, such as fluorine containing CTF (FCTF-S, F-DCBP-CTF) [15,16], acetylacetone containing CTF (acac-CTF) [17], bipyridine containing CTF (bpy-CTF) [18], ionic CTF (cCTF) [19], porphyrin CTFs [20], N-heterocyclic carbene CTF (NHC-CTF) [21], binol [22], etc. The produced

materials show good properties for several applications in gas storage and separation [23], catalysis [24], electrocatalysis [25,26], photocatalysis [27,28], and batteries [29].

However, these harsh ionothermal synthesis conditions result in materials that are mostly amorphous. In some reports, CTFs with a partial crystallinity were obtained [10,12]. Due to carbonization at these high temperatures, the structural characterization of the material becomes arduous. Nonetheless, CTFs exhibit exceptional properties in comparison to other covalent organic framework (COFs) for the above noted applications. One of the most appealing properties of the ionothermally synthesized CTFs is their exceptionally high thermal, hydrothermal, and chemical stability. They can withstand temperatures up to 550 °C and extreme chemical environments, such as 1 M NaOH or 1 M HCl solutions, for an extended period. Such stability is important for "real life" gas adsorption/separation applications, wherein high temperatures and the acid/base poisoning of the gas streams are important considerations [30]. This encouraged us to design new CTFs, particularly with polar functional sites that can be beneficial for gas storage and separations. Recently, Yaghi et al., reported the first urea-linked ketoenamine COFs and highlighted their structural dynamics with respect to their flexibility [31]. However, the COFs were not highly stable in basic conditions (1 M NaOH). In order to develop porous materials that are stable under both strong acidic and basic conditions, we report herein the synthesis of ultra-stable urea-based CTFs using a dinitrile linker, (1,3-bis(4-cyanophenyl)urea) (Scheme 1). We studied their surface properties as well as their potential for $C_2H_2$, $C_2H_4$, and $CO_2$ separation over $CH_4$. We report herein that urea-CTFs display high $C_2H_2$ and $C_2H_4$ uptakes and moderate $CO_2$ adsorption capacity in comparison to the existing CTFs. Moreover, the C2 hydrocarbon ($C_2H_2$ and $C_2H_4$) adsorption was selective compared to C1 hydrocarbon ($CH_4$). In addition, urea-CTFs also exhibited good selectivity for $CO_2$ over $CH_4$.

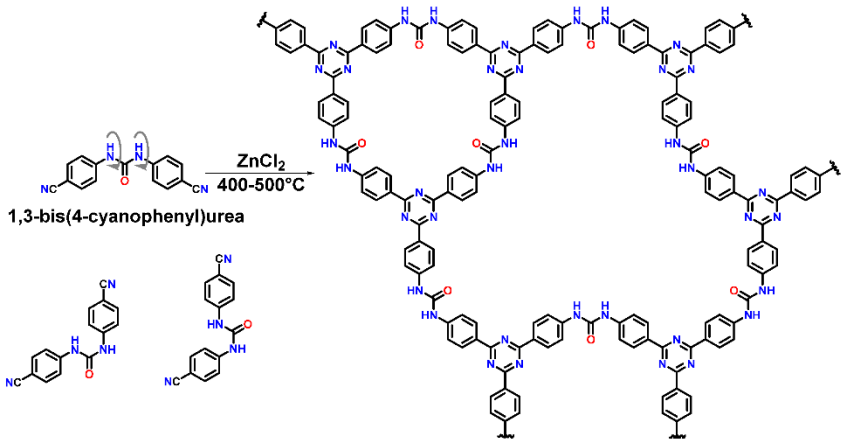


**Scheme 1.** Schematic representation of the synthesis and ideal structure of the urea-functionalized CTFs. 1,3-bis(4-cyanophenyl)urea is a flexible linker, and its possible conformations are listed.

## 2. Results and Discussion

### *2.1. Synthesis and Characterization of Urea-CTFs*

For the synthesis of the targeted urea-based CTFs, the linker 1,3-bis(4-cyanophenyl)urea was synthesized from 4-aminobenzonitrile according to the reported procedure [32]. In general, urea-CTFs were obtained through ionothermal synthesis using ZnCl2 (5 eq.) both as a catalyst and a solvent at 400 °C (urea-CTF-400-5) and 500 °C (urea-CTF-500-5) (Scheme 1, ESI). The complete trimerization of the cyano (-CN) groups was confirmed through Fourier transform infrared (FTIR) analysis (Figure S1) where the -CN peak at 2226 $cm^{-1}$ of the monomer is no longer visible in the CTFs [10,14]. In addition, triazine peaks were observed around 1360 $cm^{-1}$ and 1600 $cm^{-1}$, which further confirm the successful trimerization. Notably, a small broad peak around 1707 $cm^{-1}$ was observed in the CTFs that are red-shifted from 1737 $cm^{-1}$ of C(O) monomer and confirms the presence of urea groups in the resulting materials [31]. The observed lower wavenumber might be due to

the decrease in the double-bond character of the C(O) bond of the urea functional group after the CTF formation.

The porous properties of both the CTF materials were explored using argon sorption at 87 K (Figure 1) and $N_2$ sorption measurements at 77 K (Figure S2). Both urea-CTF_400_5 and urea-CTF_500_5 displayed a Type I isotherm typical for microporous materials, and the calculated BET surface areas were 555 $m^2$ $g^{-1}$ and 928 $m^2$ $g^{-1}$, respectively. The detailed textural properties are described in Table S1. As seen in several reported CTFs [11], the microporosity content depends on the synthesis temperature, whereas, urea-CTF_400_5 shows a higher microporous-to-mesoporous volume ratio in comparison to Urea-CTF_500_5. The theoretical expected pore sizes are 0.7 nm and 1.4–1.5 nm as shown in the structure (Scheme S1). From the experimental argon pore-size distribution, 0.75/1.43 nm pores for urea-CTF_400_5 and 1.65/2.70 nm pores for urea-CTF_500_5 were obtained. The values for urea-CTF_400_5 correspond well with the expected pore size, whereas, for urea-CTF-500, the absence of the smallest pore (0.7 nm) and the appearance of a larger pore (2.70 nm) were observed. This is the result of thermal decomposition causing the fragmentation of the walls on top of the micropores, creating mesopores in urea-CTF_500_5 [33]. A higher synthesis temperature also causes a higher degree of carbonization [34], which is seen in the C/N ratio from the elemental analysis data. The presence of a sudden drop in the adsorbed volume in the desorption isotherm at $P/P_0$~0.45 (Figure S2) is due to the tensile strength effect leading to a forced closure of the hysteresis loop [35]. The powder X-ray diffraction (PXRD) analysis show the amorphous characteristics of the materials with a broad diffraction band at 2θ = 25.8 degrees (Figure S3). The physicochemical stability of the urea-CTFs was analyzed using thermogravimetric analysis (TGA) which showed that the materials were stable up to 450 °C (Figure S4). In addition, the chemical stability of the urea-CTF_400_5 and urea-CTF_500_5 material was studied by exposing them to boiling water (3 days), 6 M NaOH (3 days), and 6 M HCl (3 days). After each treatment, they were cleaned to remove the corresponding chemical traces, and $N_2$ sorption was performed (Figures S5 and S6). In all cases, microporosity was retained, proving the permanent microporosity of the urea-CTF. Transmission electron microscopy (TEM) images show the two-dimensional stacking of the urea-CTFs (Figures S7 and S8). In addition, scanning electron microscopy (SEM) images show that urea_CTF_400_5 particles, are on average, larger than the urea_CTF_500_5 particles (Figures S7 and S8). Lower temperature synthesis of the CTF created fewer defects, and hence, urea_CTF_400_5 had longer sheet morphology.

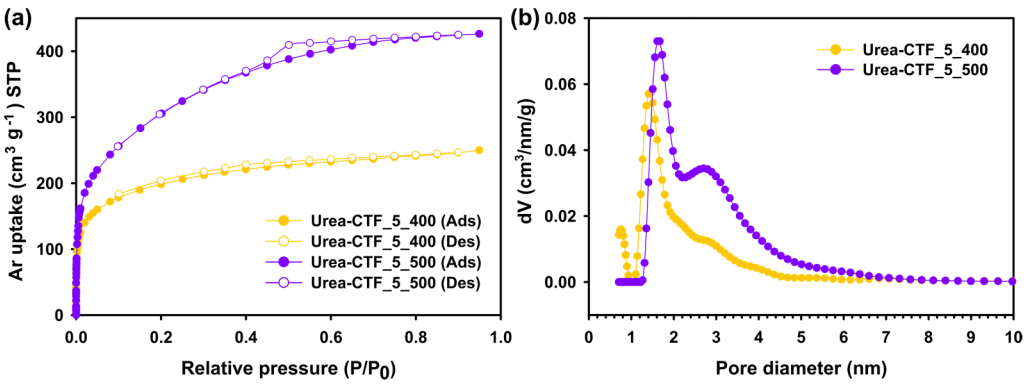


**Figure 1.** (**a**) Argon sorption isotherms measured at 87 K and (**b**) the pore-size distribution of the urea-CTFs based on quenched solid density functional theory (QSDFT) cylindrical pores.

### *2.2. Gas Storage and Separation*

Although CTFs in general have high potential for gas storage and separation, their potential for C2 hydrocarbon storage and separation has only rarely been explored. Only recently, CTF-PO71 [36] and hexene-CTF [37] have been studied for C2 hydrocarbon storage and separation. The permanent microporosity and presence of urea/triazine functional groups make urea-CTFs excellent candidates for this purpose. To this end, C2 hydrocarbon

storage capacity was tested for both urea-CTF_400_5 and urea-CTF_500_5. Among these samples, urea-CTF_400_5 showed the highest $C_2H_2$ uptake (3.86 mmol/g) at 273 K and 1 bar pressure, which is higher than the previously reported CTFs (Figure 2a).

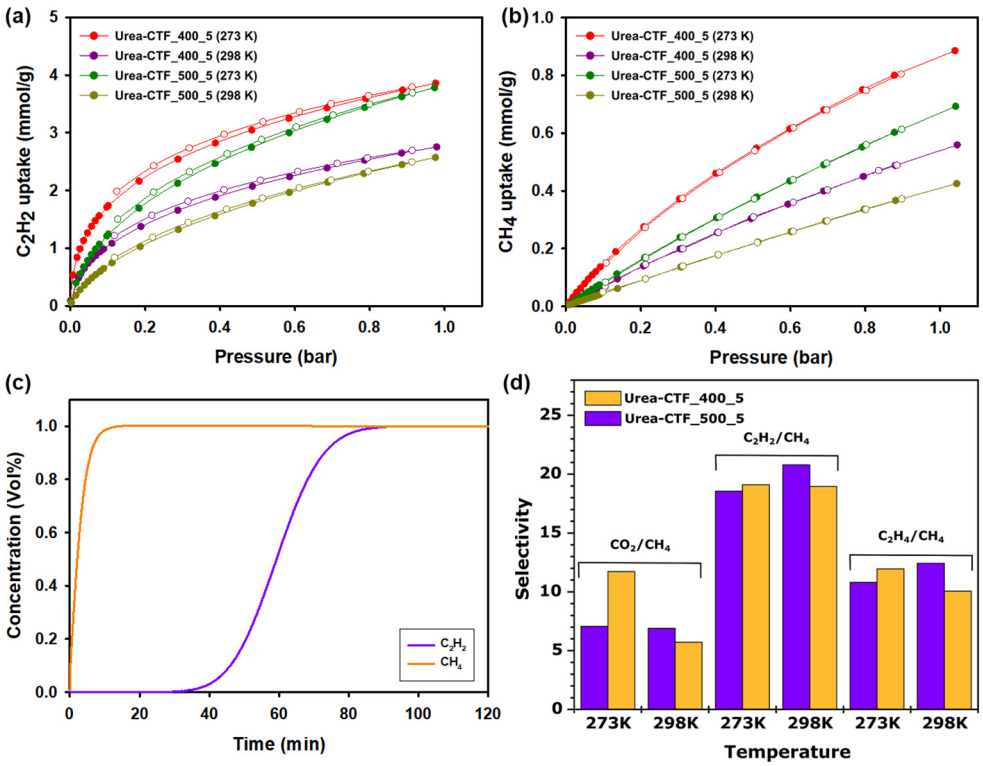


**Figure 2.** (**a**) $C_2H_2$ uptake, (**b**) $CH_4$ uptake, (**c**) $C_2H_4/CH_4$ breakthrough simulation of urea-CTF_400_5, and (**d**) $CO_2$, $C_2H_2$, and $C_2H_4$ selectivities over $CH_4$ of urea-CTF_400_5 and urea-CTF_500_5.

Interestingly, despite the higher surface area of urea-CTF_500_5, a similar $C_2H_2$ uptake (3.78 mmol/g) at 273 K and 1 bar pressure was observed (Figure 2a, Table S2). This is due to the abundance of the micropores in both materials. However, for urea-CTF_400_5, the $V_{micro}/V_{tot}$ (0.72) is slightly higher than for urea-CTF_500_5 (0.61) (Table S1). This results in a steeper increase of $C_2H_2$ uptake at the lower-pressure regime for urea-CTF_400_5. In addition, similar trends were observed in $C_2H_4$ uptake (2.89 mmol/g and 2.92 mmol/g for urea-CTF_400_5 and urea-CTF_500_5, respectively) (Figure S9). The affinity at 273 K and 298 K of the C2 hydrocarbons for the urea-CTFs was calculated by the Clausius–Clapeyron equation (Figures S11 and S12). The isosteric heat of adsorption ($Q_{st}$) values are given in Table S3. As expected, in both cases, a higher affinity was observed in urea-CTF_400_5 because the lower synthesis temperature resulted in fewer defects. In addition to the storage capacity, selectivity is perhaps an even more important parameter for industrial utilization. First, we targeted $C_2H_2/CH_4$ and $C_2H_4/CH_4$ separation. The $CH_4$ uptake isotherms at 273 K and 298 K are given in Figure 2b. Selectivity was estimated using the ideal adsorbed solution theory (IAST) (Table S4 and Figures S14–S17). The calculated selectivities of the urea-CTFs were within 16.9–20.2 and 8.9–12.4 for $C_2H_2/CH_4$ and $C_2H_4/CH_4$, respectively, which are promising results for C2/C1 hydrocarbon separation (Figure 2d, Table 1).

The presence of inherent triazine and urea functionalities in urea-CTFs also encouraged us to test $CO_2$ adsorption performance. The $CO_2$ adsorption and desorption isotherms were measured at 273 K and 298 K up to 1 bar. At 1 bar and 273 K, urea-CTF_400_5 and urea-CTF_500_5 showed 2.8 mmol/g and 3.1 mmol/g uptake respectively, which are moderate values in comparison to other CTFs (Figure S10, Table S2). The heat of liquefaction of bulk $CO_2$ is 17 kJ/mol [38], and urea-CTF_500_5 shows an isosteric heat of adsorption

of 48.57 kJ/mol (Figure S12 and Table S3), which is much higher. In addition, the $Q_{st}$ values of urea-CTFs are much higher than several reported CTFs and higher than activated carbon at low $CO_2$ pressure (17.8 kJ/mol). This confirms the strong dipolar interactions between $CO_2$ and the N-basic sites, as well as the H-bonding interactions between the urea functional group and the $CO_2$ molecules. The selectivity of $CO_2$ over $N_2$ and $CH_4$ are also important factors for CCS applications. $CO_2/CH_4$ and $CO_2/N_2$ selectivity were calculated using IAST (Table S4), and the best values, 20.3 and 69.6, were respectively obtained for urea-CTF_400_5 at 273 K. Notably, the obtained $CO_2/N_2$ selectivity of urea-CTF_400_5 is higher than several reported CTFs [14,39–41].

**Table 1.** Comparison of urea-CTFs with other materials for $C_2H_2/CH_4$ and $CO_2/CH_4$ selectivities and adsorption enthalpies.

| Material | Temp. (K) | $C_2H_2$ Uptake (mmol/g) | $C_2H_2/CH_4$ Selectivity (273 K) | $C_2H_2$ Adsorption Enthalpy (kJ/mol) | $CO_2$ Uptake (mmol/g) | $CO_2/CH_4$ Selectivity (273 K) | $CO_2$ Adsorption Enthalpy | Ref. |
|---|---|---|---|---|---|---|---|---|
| UTSA-50 | 296 | 3.80 | 68 | 39.4 | 2.63 | 5 | 27.8 | [4] |
| $Zn_4(OH)_2$(1,2,4-*btc*)$_2$ | 295 | 2.22 | 14.7 | 28.2 | 1.72 | 4.5 | 20.2 | [5] |
| ZJU-60a | 296 | 6.33 | - | 17.6 | 2.99 | 5–5.6 | 15.2 | [6] |
| Hexene-CTF_400_1 | 298 | 2.28 | 12.8 | 47 | 2.66 | 8 | 32 | [37] |
| ZJU-61a | 298 | 5.88 | 115.3 | 23.98 | - | - | - | [42] |
| HOF-BTB | 295 | 2.87 | 7.8 | 24.3 | - | - | - | [43] |
| UTSA-36a | 295 | 2.45 [Ξ] | 16.1 | 29.0 | - | - | - | [44] |
| Activated carbon | 303 | - | - | - | 3.45 | 2.5 (303 K) | 24.2 | [45] |
| Urea-CTF_400_5 | 298 | 2.80 | 20.25 | 35.51 | 1.8 | 10.49 | 30.05 | This work |
| Urea-CTF_500_5 | 298 | 2.57 | 18.96 | 27.78 | 1.5 | 10.47 | 48.57 | This work |

Note: [Ξ] Extrapolated from plot.

To verify the performance of the adsorbents in a mixed component system, breakthrough simulations were performed. Urea-CTF_400_5 was selected for these simulations as it showed the best performance among the urea-CTFs in all gas separations. The affinity constants and maximal loadings at the corresponding temperatures were obtained from Langmuir adsorption isotherm fitting (ESI). With these values, the equilibrium data for a mixed-component system were simulated. The equilibrium plots for $C_2H_2/CH_4$, $C_2H_4/CH_4$, and $CO_2/CH_4$ components with (i) constant gas composition and variable pressure and (ii) constant pressure and variable gas composition are shown in Figures S18–S20. As expected, even in a 50:50 mixtures, uptake is higher for $C_2H_2$, $C_2H_4$, and $CO_2$ as compared to $CH_4$ due to the higher affinity constants. Further breakthrough simulations were performed with defined height, diameter of the column, gas-flow rate, and mass of the adsorbent at 25 °C and 1 bar pressure. The breakthrough plots for $C_2H_2/CH_4$, $C_2H_4/CH_4$, and $CO_2/CH_4$ are shown in Figure 2c and Figures S21 and S22. The results show promising C2/C1 and $CO_2/CH_4$ separation using urea-CTF-5-400.

## 3. Conclusions

In conclusion, rigid and highly stable CTFs were synthesized using flexible urea-based linkers. These materials exhibit high surface areas with good $C_2H_2$, $C_2H_4$, and $CO_2$ adsorption properties. The calculated $C_2H_2/CH_4$, $C_2H_4/CH_4$, and $CO_2/CH_4$ selectivity values demonstrate that these materials are promising for C2/C1 hydrocarbon separation, as well as for the separation of $CO_2$ in natural gas extraction.

**Supplementary Materials:** The following are available online. Instrumentation, Synthesis of Urea-CTFs, FT-IR spectra, $N_2$ sorption, Porous properties of Urea-CTFs, PXRD pattern, TGA spectra, Stability tests, TEM and SEM images, Gas uptake values, Isosteric heat of adsorption, IAST selectivities, Breakthrough simulations. Figure S1: FT-IR spectral comparison between Urea-CTFs obtained at different temperatures with respect to the monomer, Figure S2: $N_2$ sorption isotherms of the Urea-CTFs, Figure S3: PXRD pattern of the obtained Urea-CTFs, Figure S4: TGA spectra of the obtained Urea-CTFs, Figure S5: $N_2$ sorption isotherms of (i) Urea-CTF_400_5, (ii) Urea-CTF_400_5 in boiling water for 3 days, (iii) Urea-CTF_400_5 in 6M NaOH for 3 days, and (iv) Urea-CTF_400_5 in 6M HCl for 3 days, Figure S6: $N_2$ sorption isotherms of (i) Urea-CTF_500_5, (ii) Urea-CTF_500_5 in boiling water for 3 days, (iii) Urea-CTF_500_5 in 6 M NaOH for 3 days, and (iv) Urea-CTF_500_5 in 6 M HCl for 3 days, Figure S7: TEM and SEM images of Urea-CTF_400_5, Figure S8: TEM and SEM images of Urea-CTF_500_5, Figure S9: $C_2H_4$ uptake of Urea-CTF_400_5 and Urea-CTF_500_5. Figure S10: $CO_2$ uptake of Urea-CTF_400_5 and Urea-CTF_500_5, Figure S11: Isosteric heat of adsorption ($C_2H_2$, $C_2H_4$, $CO_2$, $CH_4$, $N_2$) for the Urea-CTF_400_5, Figure S12: Isosteric heat of adsorption ($C_2H_2$, $C_2H_4$, $CO_2$, $CH_4$) for the Urea-CTF_500_5, Figure S13: $N_2$ uptake of Urea-CTF_400_5 and Urea-CTF_500_5, Figure S14: IAST selectivity of Urea-CTF_500_5 at 273 K, Figure S15: IAST selectivity of Urea-CTF_500_5 at 298 K, Figure S16: IAST selectivity of Urea-CTF_400_5 at 273 K, Figure S17: IAST selectivity of Urea-CTF_400_5 at 298 K, Figure S18: $C_2H_2$ vs $CH_4$ (mixed component simulation) at (left) constant gas composition and variable pressure and (right) variable gas composition and constant pressure, Figure S19: $C_2H_4$ vs $CH_4$ (mixed component simulation) at (left) constant gas composition and variable pressure and (right) variable gas composition and constant pressure, Figure S20: $CO_2$ vs $CH_4$ (mixed component simulation) at (left) constant gas composition and variable pressure and (right) variable gas composition and constant pressure, Figure S21: Breakthrough simulation of $C_2H_4$ vs $CH_4$ for Urea-CTF_400_5, Figure S22: Breakthrough simulation of $CO_2$ vs $CH_4$ for Urea-CTF_400_5, Scheme S1: Theoretical pore sizes in Urea-CTF, Table S1. Surface area and pore volume based on Argon sorption at 87K and elemental content of Urea- CTF, Table S2: Gas uptake values for the Urea-CTFs at 1 bar pressure, Table S3. Isosteric heat of adsorption (Qst) values for the Urea-CTFs, Table S4: IAST selectivity values of the Urea-CTFs, Table S5: Langmuir fit parameters for Urea-CTFs, Table S6: Fitting parameters of adsorption isotherms of Urea-CTF_400_5 at 298 K, Table S7: Breakthrough simulation parameters for Urea-CTF_400_5 at 298 K.

**Author Contributions:** Conceptualization, H.S.J.; methodology, C.K.; software, C.K.; validation, K.L.; formal analysis, C.K.; data curation, F.L.; writing—original draft preparation, C.K. and H.S.J.; writing—review and editing, P.V.D.V.; supervision, P.V.D.V. All authors have read and agreed to the published version of the manuscript.

**Funding:** The funding was received from Research Board of Ghent University (GOA010-17, BOF GOA2017000303).

**Institutional Review Board Statement:** Not applicable.

**Informed Consent Statement:** Not applicable.

**Data Availability Statement:** Not applicable.

**Acknowledgments:** The authors thank Katrien Haustraete for the TEM measurement.

**Conflicts of Interest:** The authors declare no conflict of interest.

**Sample Availability:** Samples of the Urea-CTFs are available from the authors.

## References

1. Rojnuckarin, A.; Floudas, C.A.; Rabitz, H.; Yetter, R.A. Methane Conversion to Ethylene and Acetylene: Optimal Control with Chlorine, Oxygen, and Heat Flux. *Ind. Eng. Chem. Res.* **1996**, *35*, 683–696. [CrossRef]
2. Bachman, J.; Kapelewski, M.; Gonzalez, M.; Reed, D.; Jaramillo, D.; Jiang, H.; Oktawiec, J.; Bloch, E.; Herm, Z.; Mason, J.; et al. *Hydrocarbon Separations in Metal-Organic Frameworks*; Abstracts of Papers American Chemical Society; American Chemical Society: Washington, DC, USA, 2019; Volume 257.
3. Maqsood, K.; Mullick, A.; Ali, A.; Kargupta, K.; Ganguly, S. Cryogenic carbon dioxide separation from natural gas: A review based on conventional and novel emerging technologies. *Rev. Chem. Eng.* **2014**, *30*, 453–477. [CrossRef]

4. Xu, H.; He, Y.B.; Zhang, Z.J.; Xiang, S.C.; Cai, J.F.; Cui, Y.J.; Yang, Y.; Qian, G.D.; Chen, B.L. A microporous metal-organic framework with both open metal and Lewis basic pyridyl sites for highly selective $C_2H_2/CH_4$ and $C_2H_2/CO_2$ gas separation at room temperature. *J. Mater. Chem. A* **2013**, *1*, 77–81. [CrossRef]
5. Zhang, Z.J.; Xiang, S.C.; Rao, X.T.; Zheng, Q.A.; Fronczek, F.R.; Qian, G.D.; Chen, B.L. A rod packing microporous metal-organic framework with open metal sites for selective guest sorption and sensing of nitrobenzene. *Chem. Commun.* **2010**, *46*, 7205–7207. [CrossRef] [PubMed]
6. Duan, X.; Zhang, Q.; Cai, J.F.; Yang, Y.; Cui, Y.J.; He, Y.B.; Wu, C.D.; Krishna, R.; Chen, B.; Qian, G.D. A new metal-organic framework with potential for adsorptive separation of methane from carbon dioxide, acetylene, ethylene, and ethane established by simulated breakthrough experiments. *J. Mater. Chem. A* **2014**, *2*, 2628–2633. [CrossRef]
7. Leus, K.; Bogaerts, T.; De Decker, J.; Depauw, H.; Hendrickx, K.; Vrielinck, H.; Van Speybroeck, V.; Van Der Voort, P. Sys-tematic study of the chemical and hydrothermal stability of selected "stable" Metal Organic Frameworks. *Microporous Mesoporous Mater.* **2016**, *226*, 110–116. [CrossRef]
8. Liu, M.; Guo, L.; Jin, S.; Tan, B. Covalent triazine frameworks: Synthesis and applications. *J. Mater. Chem. A* **2019**, *7*, 5153–5172. [CrossRef]
9. Krishnaraj, C.; Jena, H.S.; Leus, K.; Van Der Voort, P. Covalent triazine frameworks—A sustainable perspective. *Green Chem.* **2020**, *22*, 1038–1071. [CrossRef]
10. Kuhn, P.; Antonietti, M.; Thomas, A. Porous, Covalent Triazine-Based Frameworks Prepared by Ionothermal Synthesis. *Angew. Chem. Int. Ed.* **2008**, *47*, 3450–3453. [CrossRef] [PubMed]
11. Sakaushi, K.; Antonietti, M. Carbon- and Nitrogen-Based Organic Frameworks. *Acc. Chem. Res.* **2015**, *48*, 1591–1600. [CrossRef]
12. Katekomol, P.; Roeser, J.; Bojdys, M.; Weber, J.; Thomas, A. Covalent Triazine Frameworks Prepared from 1,3,5-Tricyanobenzene. *Chem. Mater.* **2013**, *25*, 1542–1548. [CrossRef]
13. Tahir, N.; Krishnaraj, C.; Leus, K.; Van Der Voort, P. Development of Covalent Triazine Frameworks as Heterogeneous Catalytic Supports. *Polymers* **2019**, *11*, 1326. [CrossRef] [PubMed]
14. Bhunia, A.; Vasylyeva, V.; Janiak, C. From a supramolecular tetranitrile to a porous covalent triazine-based framework with high gas uptake capacities. *Chem. Commun.* **2013**, *49*, 3961–3963. [CrossRef]
15. Xu, F.; Yang, S.H.; Jiang, G.S.; Ye, Q.; Wei, B.Q.; Wang, H.Q. Fluorinated, Sulfur-Rich, Covalent Triazine Frameworks for Enhanced Confinement of Polysulfides in Lithium-Sulfur Batteries. *ACS Appl. Mater. Interfaces* **2017**, *9*, 37731–37738. [CrossRef] [PubMed]
16. Wang, G.B.; Leus, K.; Jena, H.S.; Krishnaraj, C.; Zhao, S.N.; Depauw, H.; Tahir, N.; Liu, Y.Y.; Van der Voort, P. A fluo-rine-containing hydrophobic covalent triazine framework with excellent selective $CO_2$ capture performance. *J. Mater. Chem. A* **2018**, *6*, 6370–6375. [CrossRef]
17. Jena, H.S.; Krishnaraj, C.; Wang, G.; Leus, K.; Schmidt, J.; Chaoui, N.; Van Der Voort, P. Acetylacetone Covalent Triazine Framework: An Efficient Carbon Capture and Storage Material and a Highly Stable Heterogeneous Catalyst. *Chem. Mater.* **2018**, *30*, 4102–4111. [CrossRef]
18. Park, K.; Gunasekar, G.H.; Prakash, N.; Jung, K.-D.; Yoon, S. A Highly Efficient Heterogenized Iridium Complex for the Catalytic Hydrogenation of Carbon Dioxide to Formate. *ChemSusChem* **2015**, *8*, 3410–3413. [CrossRef] [PubMed]
19. Buyukcakir, O.; Je, S.H.; Talapaneni, S.N.; Kim, D.; Coskun, A. Charged Covalent Triazine Frameworks for $CO_2$ Capture and Conversion. *ACS Appl. Mater. Interfaces* **2017**, *9*, 7209–7216. [CrossRef]
20. Ma, H.; Ren, H.; Meng, S.; Sun, F.; Zhu, G. Novel Porphyrinic Porous Organic Frameworks for High Performance Separation of Small Hydrocarbons. *Sci. Rep.* **2013**, *3*, srep02611. [CrossRef]
21. Gunasekar, G.H.; Park, K.; Ganesan, V.; Lee, K.; Kim, N.K.; Jung, K.D.; Yoon, S. A Covalent Triazine Framework, Functionalized with Ir/N-Heterocyclic Carbene Sites, for the Efficient Hydrogenation of $CO_2$ to Formate. *Chem. Mater.* **2017**, *29*, 6740–6748. [CrossRef]
22. Jena, H.S.; Krishnaraj, C.; Parwaiz, S.; Lecoeuvre, F.; Schmidt, J.; Pradhan, D.; Van Der Voort, P. Illustrating the Role of Quaternary-N of BINOL Covalent Triazine-Based Frameworks in Oxygen Reduction and Hydrogen Evolution Reactions. *ACS Appl. Mater. Interfaces* **2020**, *12*, 44689–44699. [CrossRef]
23. Jena, H.S.; Krishnaraj, C.; Schmidt, J.; Leus, K.; Van Hecke, K.; Van Der Voort, P. Effect of Building Block Transformation in Covalent Triazine-Based Frameworks for Enhanced $CO_2$ Uptake and Metal-Free Heterogeneous Catalysis. *Chem. Eur. J.* **2020**, *26*, 1548–1557. [CrossRef]
24. Chan-Thaw, C.E.; Villa, A.; Katekomol, P.; Su, D.S.; Thomas, A.; Prati, L. Covalent Triazine Framework as Catalytic Support for Liquid Phase Reaction. *Nano Lett.* **2010**, *10*, 537–541. [CrossRef]
25. Laemont, A.; Abednatanzi, S.; Derakshandeh, P.G.; Verbruggen, F.; Fiset, E.; Qin, Q.; Van Daele, K.; Meledina, M.; Schmidt, J.; Oschatz, M.; et al. Covalent triazine frame-work/carbon nanotube hybrids enabling selective reduction of $CO_2$ to CO at low overpotential. *Green Chem.* **2020**, *22*, 3095–3103. [CrossRef]
26. Yoshioka, T.; Iwase, K.; Nakanishi, S.; Hashimoto, K.; Kamiya, K. Electrocatalytic Reduction of Nitrate to Nitrous Oxide by a Copper-Modified Covalent Triazine Framework. *J. Phys. Chem. C* **2016**, *120*, 15729–15734. [CrossRef]
27. Kuecken, S.; Acharjya, A.; Zhi, L.; Schwarze, M.; Schomäcker, R.; Thomas, A. Fast tuning of covalent triazine frameworks for photocatalytic hydrogen evolution. *Chem. Commun.* **2017**, *53*, 5854–5857. [CrossRef]
28. Schwinghammer, K.; Hug, S.; Mesch, M.B.; Senker, J.; Lotsch, B.V. Phenyl-triazine oligomers for light-driven hydrogen evolution. *Energy Environ. Sci.* **2015**, *8*, 3345–3353. [CrossRef]

29. Li, Y.; Zheng, S.; Liu, X.; Li, P.; Sun, L.; Yang, R.; Wang, S.; Wu, Z.; Bao, X.; Deng, W. Conductive Microporous Covalent Triazine-Based Framework for High-Performance Electrochemical Capacitive Energy Storage. *Angew. Chem. Int. Ed.* **2018**, *57*, 7992–7996. [CrossRef] [PubMed]
30. Rogge, S.M.J.; Bavykina, A.; Hajek, J.; Garcia, H.; Olivos-Suarez, A.I.; Sepúlveda-Escribano, A.; Vimont, A.; Clet, G.; Bazin, P.; Kapteijn, F.; et al. Metal–organic and covalent organic frameworks as single-site catalysts. *Chem. Soc. Rev.* **2017**, *46*, 3134–3184. [CrossRef] [PubMed]
31. Zhao, C.; Diercks, C.S.; Zhu, C.; Hanikel, N.; Pei, X.; Yaghi, O.M. Urea-Linked Covalent Organic Frameworks. *J. Am. Chem. Soc.* **2018**, *140*, 16438–16441. [CrossRef] [PubMed]
32. Wang, M.; Han, J.; Si, X.; Hu, Y.; Zhu, J.; Sun, X. Effective approach to ureas through organocatalyzed one-pot process. *Tetrahedron Lett.* **2018**, *59*, 1614–1618. [CrossRef]
33. Osadchii, D.Y.; Olivos-Suarez, A.I.; Bavykina, A.V.; Gascon, J. Revisiting Nitrogen Species in Covalent Triazine Frameworks. *Langmuir* **2017**, *33*, 14278–14285. [CrossRef]
34. Kuhn, P.; Forget, A.; Hartmann, J.; Thomas, A.; Antonietti, M. Template-Free Tuning of Nanopores in Carbonaceous Polymers through Ionothermal Synthesis. *Adv. Mater.* **2009**, *21*, 897–901. [CrossRef]
35. Groen, C.J.; Peffer, A.A.L.; Pérez-Ramírez, J. Pore Size Determination in Modified Micro- and Mesoporous Materials. Pitfalls and limitations in gas adsorption data analysis. *Microporous Mesoporous Mater.* **2003**, *60*, 1–17. [CrossRef]
36. Lu, Y.; He, J.; Chen, Y.L.; Wang, H.; Zhao, Y.F.; Han, Y.; Ding, Y. Effective Acetylene/Ethylene Separation at Ambient Conditions by a Pigment-Based Covalent-Triazine Framework. *Macromol. Rapid Commun.* **2018**, *39*, 1700468. [CrossRef] [PubMed]
37. Krishnaraj, C.; Jena, H.S.; Leus, K.; Freeman, H.M.; Benning, L.G.; Van Der Voort, P. An aliphatic hexene-covalent triazine framework for selective acetylene/methane and ethylene/methane separation. *J. Mater. Chem. A* **2019**, *7*, 13188–13196. [CrossRef]
38. Keskin, S.; Van Heest, T.M.; Sholl, D.S. Can Metal-Organic Framework Materials Play a Useful Role in Large-Scale Carbon Dioxide Separations? *ChemSusChem* **2010**, *3*, 879–891. [CrossRef]
39. Yuan, K.; Liu, C.; Zong, L.; Yu, G.; Cheng, S.; Wang, J.; Weng, Z.; Jian, X. Promoting and Tuning Porosity of Flexible Ether-Linked Phthalazinone-Based Covalent Triazine Frameworks Utilizing Substitution Effect for Effective $CO_2$ Capture. *ACS Appl. Mater. Interfaces* **2017**, *9*, 13201–13212. [CrossRef]
40. Park, K.; Lee, K.; Kim, H.; Ganesan, V.; Cho, K.; Jeong, S.K.; Yoon, S. Preparation of covalent triazine frameworks with imidazolium cations embedded in basic sites and their application for $CO_2$ capture. *J. Mater. Chem. A* **2017**, *5*, 8576–8582. [CrossRef]
41. Tao, L.M.; Niu, F.; Liu, J.G.; Wang, T.M.; Wang, Q.H. Troger's base functionalized covalent triazine frameworks for $CO_2$ capture. *RSC Adv.* **2016**, *6*, 94365–94372. [CrossRef]
42. Duan, X.; Zhang, Q.; Cai, J.; Cui, Y.; Wu, C.; Yang, Y.; Qian, G. A new microporous metal–organic framework with potential for highly selective separation methane from acetylene, ethylene and ethane at room temperature. *Microporous Mesoporous Mater.* **2014**, *190*, 32–37. [CrossRef]
43. Yoon, T.-U.; Bin Baek, S.; Kim, D.; Kim, E.-J.; Lee, W.-G.; Singh, B.K.; Lah, M.S.; Bae, Y.-S.; Kim, K.S. Efficient separation of C2 hydrocarbons in a permanently porous hydrogen-bonded organic framework. *Chem. Commun.* **2018**, *54*, 9360–9363. [CrossRef] [PubMed]
44. Das, M.C.; Xu, H.; Xiang, S.; Zhang, Z.; Arman, H.D.; Qian, G.; Chen, B. A New Approach to Construct a Doubly Interpenetrated Microporous Metal-Organic Framework of Primitive Cubic Net for Highly Selective Sorption of Small Hydrocarbon Molecules. *Chem. Eur. J.* **2011**, *17*, 7817–7822. [CrossRef] [PubMed]
45. Sircar, S.; Golden, T.; Rao, M. Activated carbon for gas separation and storage. *Carbon* **1996**, *34*, 1–12. [CrossRef]